Title

Magnetic Cytoskeleton Affinity Purification of Microtubule Motors Conjugated to Quantum Dots

Journal

Bioconjugate Chemistry, 29(7)

ISSN

1043-1802

Authors

Tjioe, Marco
Ryoo, Hyeon
Ishitsuka, Yuji
et al.

Publication Date

2018-07-18

DOI

10.1021/acs.bioconjchem.8b00264

Peer reviewed

HHS Public Access

Author manuscript

Bioconjug Chem. Author manuscript; available in PMC 2019 July 18.

Published in final edited form as:

Bioconjug Chem. 2018 July 18; 29(7): 2278–2286. doi:10.1021/acs.bioconjchem.8b00264.

Magnetic Cytoskeleton Affinity (MiCA) Purification of Microtubule Motors conjugated to Quantum Dots

Marco Tjioe[1,2,3], **Hyeon Ryoo**[2,4], **Yuji Ishitsuka**[2,3], **Pinghua Ge**[2,3], **Carol Bookwalter**[4], **Walter Huynh**[5], **Richard J. McKenney**[6], **Kathleen M. Trybus**[4], and **Paul R. Selvin**[1,2,3]

[1]Center for Biophysics and Computational Biology, University of Illinois at Urbana-Champaign, Urbana, Illinois 61801, United States

[2]Center for the Physics of Living Cells, University of Illinois at Urbana-Champaign, Urbana, Illinois 61801, United States

[3]Department of Physics, University of Illinois at Urbana-Champaign, Urbana, Illinois 61801, United States

[4]Bioengineering and Biomedical Engineering, University of Illinois at Urbana-Champaign, Urbana, Illinois 61801, United States, and Department of Molecular Physiology and Biophysics, University of Vermont, Burlington, VT 05405

[5]Dept. of Cellular and Molecular Pharmacology, University of California San Francisco, San Francisco, CA 94143

[6]Molecular & Cellular Biology, University of California, Davis, La Jolla, CA 92093

Abstract

We develop Magnetic Cytoskeleton Affinity (MiCA) purification, which allows for rapid isolation of molecular motors conjugated to large multivalent quantum dots, in miniscule quantities, which is especially useful for single-molecule applications. When purifying labeled molecular motors, an excess of fluorophores or labels is usually used. However, large labels tend to sediment during the centrifugation step of microtubule affinity purification, a traditionally powerful technique for motor purification. This is solved with MiCA, and purification time is cut from 2 hours to 20 minutes, a significant time-savings when it needs to be done daily. For kinesin, MiCA works with as little as 0.6 μg protein, with yield of ~27%, compared to 41% with traditional purification. We show the utility of MiCA purification in a force-gliding assay with kinesin, allowing, for the first time, simultaneous determination of whether the force from each motor in a multiple-motor system drives or hinders microtubule movement. Furthermore, we demonstrate rapid purification of just 30 ng dynein-dynactin-BICD2N-QD (DDB-QD), ordinarily a difficult protein-complex to purify.

Supporting Information

Supporting Information is available.

Introduction

Kinesin, dynein, and myosin are cytoskeletal motor proteins that convert chemical energy into mechanical work to power much of the movements within the cell. They are responsible for a wide range of motion inside the cell from membrane trafficking to movement of the entire cell[1]. Their defects are implicated in many diseases[2–11].

Single molecule studies offer powerful means to uncover mechanisms of motor movements, allowing examination of the step-sizes[12–20] and forces[17,19,21–25] generated by a single motor. A recurring challenge in single molecule studies is ensuring that measurements are done on one motor. This is challenging with large labels as they tend to be multivalent, and thus can attach to multiple motors. A common solution is to mix excess labels per motor[26–32], but this procedure contributes to noise and increase unproductive events, adversely affecting single molecule analysis.

To remove excess labels and obtain active microtubule-based motors, many laboratories use the well-established microtubule affinity purification[33–37]. In this method, motors bind to and are subsequently released from microtubules with the addition of ATP, while excess labels remain unbound and are washed away after centrifugation. It has been applied to purify unlabeled motors from cellular extract[34,38], and motors bound to fluorescent proteins[39] and organic fluorophores[14,33]. It is, however, unable to purify motors labeled with large labels, as excess labels sediment during the high speed centrifugation, preventing their separation from labeled motors. To our knowledge, no purification has been done on motors labeled to reporters larger than 10 nm, even though a significant number of studies have made use of large reporters—especially quantum dots (QD)[26–28,30–32,40,41], due to quantum dots brightness and photostability.

The other drawbacks of microtubule affinity purification include the use of a large quantity of samples (μg to mg) and long purification time (a few hours). These are not optimal for single molecule study, since only a small amount of sample is needed for each experiment, and conjugated motors may have a short lifetime before dissociating or becoming inactive.

To address these drawbacks, we developed Magnetic Cytoskeleton Affinity (MiCA) purification, which uses magnetic separation technology[42,43], instead of a centrifugation step (Figure 1). In short, microtubules are immobilized on magnetic beads, and then labeled-motors bind to, and release from, the immobilized microtubules using different ATP analogues. The result is isolated motors labeled with quantum dots, free of any unlabeled quantum dots and inactive motors incapable of binding microtubules. The key to a robust MiCA purification is to use moderately positive magnetic beads with long PEG chain, as shown in Figure 2. This works well as the positively charged bead binds strongly to negatively charged microtubules, while the PEG chain effectively prevents non-specific interaction with motors, allowing motors to bind and release.

Here we demonstrate the efficacy of MiCA purification on kinesin bound to QD, on kinesin-only for comparison with traditional microtubule affinity purification, and on dynein-dynactin-BICD2N (DDB) complex bound to QD. It takes only 20 minutes to complete MiCA purification, a significant time saving from the 2 hours needed for microtubule

affinity purification. The yield for MiCA purification is ~27%, and we have successfully purified active kinesin-QD and DDB-QD in minute quantities, 340 ng and 30 ng respectively. Lastly, we demonstrate an application for purified kinesin-QD using force-gliding assay, where, for the first time, the forces of multiple kinesin can be detected simultaneously.

Results and Discussion

MiCA purification protocol

MiCA purification is derived from the traditional microtubule affinity purification. The experimental protocols for both are illustrated in Figure 1, highlighting how MiCA purification can be used to separate motors labeled with large fluorophore from inactive and excess fluorophores, while traditional purification cannot. A detailed protocol for traditional microtubule affinity purification can be found in Supporting Information section 2. The magnetic separation (step 3 and 5) for MiCA purification replaces centrifugation used in traditional purification. Below are the six steps of MiCA purification:

1. MiCA capture beads are formed by mixing short microtubules with moderately positive magnetic beads:
   - Short microtubules (< 1 μm) are polymerized from 5 mg/mL tubulin at 37°C for 30 mins in the presence of 2 mM GMPCPP (non-hydrolysable analog of GTP), then sonicated for 3 mins
   - Long microtubules can also be used for MiCA purification, but short ones are preferable to allow long term storage and prevent aggregation of motors, as discussed in Supplementary Information section 1
2. MiCA capture beads are mixed with the motor sample in the presence of 1 mM AMP-PNP:
   - Three different species are illustrated in Figure 1: excess big probe, probe-bound active kinesin, and probe-bound inactive kinesin. MiCA purification removes the excess big probe and probe-bound inactive kinesin
3. MiCA capture beads are pulled by a magnet positioned outside of reaction tube, leaving excess big probe and probe-bound inactive kinesin in the supernatant.
4. The supernatant is removed, and the pellet is washed with dilution buffer 2–3 times, and then eluted with 1–3 mM ATP, which releases probe-bound active kinesin from MiCA capture beads.
5. MiCA capture beads are again pulled by magnet, leaving probe-bound active kinesin in the supernatant.
6. The supernatant is transferred to a new centrifuge tube separate from the pellet.

Magnetic beads preparation

An important element to the robustness of MiCA purification is the magnetic beads used to bind microtubules. We use charge interaction to couple positively charged amine beads to the negatively charged microtubules. However, we find that commercial amine beads are too positively charged: they will bind strongly not only to microtubule but also to kinesin, preventing kinesin from being eluted. We therefore reduce the positive charge on the beads by coupling PEG-amine, resulting in moderately positive beads that bind to microtubule, but not kinesin. The synthesis of this PEG-amine bead is illustrated in Figure 2(A), with detailed protocol outlined in Supporting Information section 3.1. Briefly, commercial amine beads are washed with double-distilled water (ddH_2O), and then reacted with FMOC-NH-PEG-SVA (Laysan Bio, Inc.). The reaction yields FMOC-coated beads, which is washed with ddH_2O. The FMOC beads are then deprotected with piperidine[44], yielding amine (NH_2) in place of FMOC-NH group, generating PEG-amine bead. These beads can be stored at 4°C and are good for at least six months.

Figure 2(B) summarizes the result of an SDS-PAGE electrophoresis binding experiment, showing that amine beads bind strongly to both kinesin and microtubule, while PEG-amine beads bind preferentially to microtubule but not kinesin. Detailed experimental protocol is described in Supporting Information section 3.2. Briefly, kinesin and microtubules are separately mixed with amine or PEG-amine bead, and the proteins left in supernatant (Sup) or stuck on final bead (Bead) are monitored. The binding of kinesin and microtubules to amine beads are so strong that no protein is detected in the supernatant shown on lane 2 and no protein is released from beads shown on lane 3 even after mixing with SDS detergent and heated to 95°C. With PEG-amine bead, kinesin binding is minimized, as a significant amount of kinesin remains in the supernatant shown on lane 4, and only a small fraction then stick to PEG-amine beads shown on lane 5. PEG-amine beads still preserve its ability to bind microtubules, as only a small fraction of microtubules remain in the supernatant shown on lane 4, but a large fraction stick to PEG-amine beads shown on lane 5. We perform a control experiment using BSA to block amine and PEG-amine beads, and the result is the same for the PEG-amine beads. This result is summarized in Supporting Figure S1.

Figure 2(C) shows Total Internal Reflection Fluorescence (TIRF) imaging of kinesin-QD and fluorescent microtubules binding to amine and PEG-amine surfaces, providing further support that amine surfaces bind strongly to both kinesin-QD and microtubules, but PEG-amine surfaces bind only to microtubules. Detailed experiment is outlined in Supporting Information section 3.3. Control experiment summarized in Supporting Figure S2 shows that as PEG-amine concentration on the surface is reduced, fewer microtubules bind, confirming that binding of the microtubules to the surface is through presence of PEG-amine. Another control experiment shown in Supporting Figure S3 and Supporting Movie S3 concludes that kinesin-QD moves well on microtubules adhered to the PEG-amine surface (around 70% are motile) but not amine surface (only around 26% are motile).

Attempts to generate MiCA capture beads using other conjugation schemes failed and are discussed in Supporting Information section 3.3. In general, a good MiCA capture bead should bind strongly to microtubules, but not the motors being purified. The first experiment to run is therefore binding tests for microtubules and motors to the magnetic beads.

MiCA reduces purification time sevenfold

Figure 3(A) summarizes the time needed for traditional affinity vs. MiCA purification. Total purification time reduces from 130 mins for traditional affinity to 19 mins for MiCA purification. Initial microtubule polymerization and centrifugation step that takes 60 mins in traditional affinity is replaced with a 5-min MiCA capture bead preparation using short microtubules stored at −80°C. The binding and elution step takes the same time for both traditional affinity and MiCA purification, but the wash and eluant extraction are 15 times faster for MiCA than for traditional affinity purification. This is because the 30-min centrifugation time in traditional affinity is replaced with a 2-min magnetic separation in MiCA purification. Note that the 60-min initial polymerization and centrifugation step for traditional affinity protocol can be shortened to 30 mins by doing batch polymerization, aliquoting and storing at −80°C, and then start only from 30-min centrifugation to remove short microtubules, as outlined in Supporting Information section 2. This will reduce the traditional affinity purification time from 130 mins to 100 mins, which is five times longer than that of MiCA purification.

MiCA delivers 27% kinesin yield

Figure 3(B–C) shows traditional affinity and MiCA purification experiments monitored through SDS gel electrophoresis. Detailed protocol for this experiment can be found in Materials and Methods. The yield for each is shown on the Elute lane. The yield for MiCA is 27%, 1.5x less than that of traditional affinity purification, which is 41%. The initial protein amount is shown on the first lane. This initial kinesin binds to the microtubules (for traditional) or magnetic bead (for MiCA) by the addition of AMP-PNP. The second lane (AMP) shows the amount of protein left in the supernatant and not binding to the microtubules or magnetic bead. Most kinesin bind to the microtubules or magnetic beads. Only 8% and 4% of kinesin are left in supernatant for traditional affinity and MiCA purification. After the binding step, the kinesin-bound microtubules or magnetic beads are washed. The wash lane shows that minimal protein is lost (2% and 4%) at this step. Once washed, the kinesin is eluted with ATP, and both the amount eluted and amount left in beads are monitored in the Elute and Left lane. The amount eluted (41% and 27%) are comparable to the amount left on microtubules or magnetic beads (36% and 30%). A second elution step can be added to increase the final yield if desired.

MiCA allows single molecule observation of kinesin-QD in a microtubule gliding assay through removal of free dyes

Microtubule gliding assays generally have unlabeled kinesin bound to the surface-moving microtubules. Current effort to visualize kinesin in a gliding assay is limited to “spiking” experiments, where high concentration of unlabeled kinesin are laid down and spiked with low concentration of GFP-labeled kinesin[45]. These experiments suffer from the low photostability of GFP and the inability to track all the kinesin on the surface. With MiCA purification of kinesin-QD, all kinesin-QD can now be tracked, and for a very long time owing to the photostability of the QDs.

Figure 3(D–G) shows microtubule gliding experiments using kinesin-QD before and after MiCA purification. This is also shown in Supporting Movie S1. Detailed protocol for this

experiment can be found in Materials and Methods. Figure 3(E) shows fluorescence of QD (magenta) and microtubule (blue) overlaid with green dots to mark location of QDs with active kinesin. QDs are considered active if they co-localize with microtubule for at least 8 frames (16 seconds). Kinesin is mixed with QD in 1 to 1.1 ratio. At this ratio, some QDs (~23%) will have two or more kinesin bound, and since they will be present before and after MiCA purification, it is not critical for all QDs to be singly labeled with kinesin. Before MiCA purification, free QDs (statistically ~40%) and QDs with inactive kinesin are not removed. Figure 3(F) shows that at the end of the gliding experiment, only 20% of QDs before MiCA purification are actively gliding microtubules, compared to 60% are after MiCA purification. Figure 3(G) shows that at any period of time the fraction of QDs with active kinesin after MiCA are approximately 3 times higher than before MiCA.

MiCA enables force-gliding assay for parallel detection of forces from multiple kinesin

Here we show a proof-of-principle of force-gliding assay made possible by MiCA purification. This assay allows simultaneous detection of forces from multiple kinesin for the first time. The experiment setup is similar to the microtubule gliding assay with kinesin-QD shown in Figure 3(D), with the addition of a 1,565 base-pair double-stranded DNA between the kinesin-QD and the biotin-PEG coverslip, as shown in Figure 4(A). The DNA acts as a spring that allows force detection of kinesin-QD as it drives or hinders microtubule. Driving kinesin moves in the opposite direction of microtubule, while hindering kinesin moves in the same direction. Detailed protocol for this experiment can be found in Materials and Methods. Our current setup allows accurate detection of direction but not magnitude of the force exerted by kinesin on microtubule (see Supporting Information section 16 for discussion on force accuracy).

Figure 4(B) shows snippets of force-gliding assay from Supporting Movie S4 at 2.6, 12.8, 21.8 and 35.0 seconds. Two kinesin move microtubule (green). White arrows show equilibrium kinesin positions. Red arrow shows the direction of microtubule movement. As microtubule glides over kinesin, the two kinesin are seen driving or hindering microtubule at different times.

Figure 4(C) shows plots of microtubule velocity and kinesin positions over time. Time-points at 2.6, 12.8, 21.8 and 35.0 s corresponding to the images in (B) are marked with yellow vertical line. At 2.6 s, microtubule velocity is ~0 nm/s and no kinesin is attached. At 12.8 s, microtubule velocity increases to 800 nm/s when both kinesin are driving (downward displacement from equilibrium). At 21.8 s, top kinesin remains driving, while bottom kinesin hinders microtubule, causing microtubule velocity to fall to 400 nm/s. At 35.0 s, microtubule glides past bottom kinesin, and top kinesin becomes the sole driver, moving microtubule at 800 nm/s.

MiCA allows purification of as little as 30 ng DDB bound to QD

Dynein-dynactin-BICD2N (DDB) complex is difficult to isolate and its purification yield is typically much lower than that of kinesin. It has recently been of interest because binding of BICD2N allows dynein-dynactin to be ultra-processive[46,47] and increases its force

production four fold[33]. In our hands, DDB needs to be mixed with 5–10x more QD in molar ratio, in order to bind (non-specifically) to QD.

Our successful purification of DDB-QD with MiCA demonstrates that MiCA is able to purify very small quantity of a traditionally challenging protein (30 ng), and that a large excess of QD (5–10x) can be removed with MiCA, significantly increasing the pool of active DDB-QD. Detailed protocol for MiCA purification of DDB-QD and its quantification using TIRF microscopy are laid out in Materials and Methods. Figure 5 shows the result of successful purification of DDB-QD. Optimization experiment for DDB-QD is described in Supporting Information section 13.

Figure 5(A–B) show TIRF images and kymographs of DDB-QD purification. The amount of DDB-QD left after binding to MiCA capture beads (Sup), left in second wash (Wash 2), and eluting through first and second elution (Elute 1 and 2) are shown in (A) and quantified in (C). Total yield including Elute 1 and 2 is 25%. Free QDs and unbound DDB-QDs contribute to high background noise in Sup. After 2 wash cycles, they are removed, as shown by the low background noise in Wash 2, Elute 1 and Elute 2. Figure 5(B) show kymographs of DDB-QDs, which are stationary or diffusive in Sup and Wash 2, but processive in Elute 1 and 2. This is also shown in Supporting Movie S2.

To quantify the extent to which excess QDs are removed, we look at the background created by the excess QD, which will reduce the signal to noise ratio (SNR) and worsen the spatial precision of DDB-QD after fitting a 2D Gaussian and analyzed using FIONA[48]. The SNR is the ratio between the peak and base of the 2D Gaussian fit, and the spatial precision calculation using FIONA takes into account the number of photons, finite pixel size, and background. Figure 5(D) compares the SNR and precision obtained from QDs before (Sup) and after MiCA (Elute 1). The SNR before MiCA (11) is 5x less than after MiCA (55). The spatial precision achieved before MiCA (17 nm) is ~3x worse than after MiCA (5 nm).

Optimizing MiCA purification

Discussions on the general strategy for MiCA purification and its limitations are outlined in Supporting Information section 17 and 18.

Conclusions

MiCA purification is ideal for point-of-use purification of molecular motor either by itself or attached to a cargo. It is fast and able to purify small quantity of motors. In this paper, we show successful purification of kinesin, kinesin-QD and DDB-QD with MiCA. The purification yield is as high as 27%, and it is able to purify as little as 30 ng DDB-QD. We also demonstrate a proof-of-principle of force-gliding assay, which allows parallel force detections from multiple kinesin-QDs for the first time. MiCA purification shortens purification time from 2 hours to 20 minutes, lending itself to routine purification of conjugated motors for a wide-range of single molecule and biomolecular experiments. It is expected to be widely useful, although one must be aware of the disruption of cytoskeleton binding to the PEG-amine magnetic bead due to high salt and casein. In addition, it may be possible to extend this procedure to cell extracts.

Materials and Methods

Preparation of kinesin

Three different types of kinesin are used. All of them are truncated kinesin with biotin attached either to the C-terminus where the cargo binding domain of full length kinesin lies, or the N-terminus where the catalytic domain lies. The shortest kinesin used is K432, a 432 amino-acid fraction of *Drosophila* kinesin. The next two kinesin, K888 and K888-Het, are equally long with 888 amino acids from the mouse kinesin heavy chain. K888 is a homodimer with biotin on the C terminus of both monomers, while K888-Het is a heterodimer with biotin on the N-terminus of only one of the two monomers. The preparation of all kinesin is detailed in Supporting Information section 11.

Preparation of dynein-dynactin-BICD2N (DDB) complex

DDB was prepared from porcine brain lysate[46,47]. Briefly, fresh porcine brain was obtained from the slaughterhouse. They were then cut into small pieces and frozen into batch aliquots. When needed, a fresh batch of lysate was prepared by thawing an aliquot at 37°C and homogenizing in a 1:1 ratio with 50 mM Hepes, 50 mM Pipes pH 7.0, 1 mM EDTA, and 2 mM $MgSO_4$ in a Waring blender. The lysate was then transferred to a glass douncer and further homogenized with a Teflon pestle. This was followed by a 30 minute spin at 30,000 × *g*. Lysates were flash frozen in 2 mL aliquots at this point. Prior to performing the DDB pull-down assay, aliquots were thawed and further clarified at 100,000 × *g* for 10 min before use. For purifying DDB, 500 μL of porcine brain lysate was mixed together with BICD2N[47] to a final concentration of 100 nM and 100 μL of a 50% Strep-tactin Sepharose bead slurry (GE Healthcare). NP-40, PMSF, and DTT were added to a final concentration of 0.1%, 1 mM, and 5 mM respectively. The mixture was incubated while rotating for 1 hour at 4°C and then washed 4 times with Buffer A (30 mM Hepes, pH 7.4, 50 mM potassium acetate, 2 mM magnesium acetate, 1 mM EGTA, and 10% glycerol) containing 0.1% NP-40 and 5 mM DTT. The DDB complexes were then eluted by incubating the beads with 100 μL of Buffer A containing 2.5mM of desthiobiotin. Sucrose was added to a final concentration of 6%, and the DDB were then flash frozen as aliquots.

Kinesin purification with microtubule affinity and MiCA purification monitored using gel electrophoresis

Long microtubules are prepared by polymerizing 8 μL tubulin (5 mg/mL) in 1 mM GMP-CPP for 30 minutes at 37°C. 15 μL GMP-Taxol buffer (20 μM paclitaxel, 1 mM GMP-CPP in BRB80) is then added and the solution is divided into 2 tubes of 10 μL each. One tube is centrifuged for 30 mins at 13,000×g, and then reconstituted in 10 μL GMP-Taxol buffer to make the long microtubules. The other tube is sonicated for 3 min at room temperature to make the short microtubules. Any buffer coming into contact with microtubules should be warmed to room temperature.

MiCA capture bead is prepared by removing the buffer in 50 μL PEG-amine bead (10 mg/mL) and mixing in 6.25 μL short microtubules. The mixture is left to incubate for 5 min, and reconstituted in 5 μL dilution taxol buffer (20 μM paclitaxel, 1 mM THP, and 80 nM ATP in DmB - dynein motility buffer: 30 mM HEPES, 50 mM KAcetate, 2 mM MgAcetate,

1 mM EGTA, pH 7.2). 5 μL DmB-BSA is then added, and the mixture incubated for 2 min followed by washing with 10 μL dilution taxol buffer. Finally the beads are reconstituted in 5 μL dilution taxol buffer to make a final volume of ~6 μL.

K888-Het is diluted 4x to ~3.75 μM in dilution-taxol buffer. For traditional affinity purification, 1 μL of this diluted K888-Het is mixed with 3.5 μL long microtubules, 1 μL AMP-PNP (8 mM), and 2.5 μL dilution taxol buffer. For MiCA purification, 1 μL K888-Het (3.75 μM) is mixed with 6 μL MiCA capture bead and 1 μL AMP-PNP (8 mM). The mixtures are incubated for 5 min at room temperature in an end-to-end rotator.

The kinesin-microtubule and kinesin-bead are washed with 8 μL dilution taxol buffer twice. For traditional affinity purification, washing is done by centrifuging mixture at 13,000×g for 30 mins at room temperature to pellet the kinesin-microtubule, and then gently add and remove dilution taxol buffer without disturbing the pellet. For MiCA purification, washing is done by magnetic separation to pellet the kinesin-bead, then the buffer is removed and the pellet reconstituted in dilution taxol buffer.

Once washed, the pellets are reconstituted in 8 μL elution buffer (3 mM ATP in dilution taxol buffer) and left to incubate for 5 min. The eluants are collected through centrifugation or magnetic separation, and another 8 μL elution buffer is added and incubated for 5 min. The second batches of eluants are again collected.

The AMP-PNP supernatant, two wash batches, two elution batches, and proteins left in bead or pellet are then quantified with SDS-PAGE electrophoresis using Imperial™ protein stain (Cat. 24615, ThermoFisher Scientific).

Microtubule gliding assay with kinesin-QD after MiCA purification

Kinesin-QD is prepared by mixing 0.2 μL K888 (8.8 μM, or 640 ng with molecular weight of 360 kDa per kinesin dimer), 1 μL Qdot® 655 Streptavidin Conjugate (SA-Qd655, 1 μM), and 1.8 μL BSA-taxol buffer (20 μM paclitaxel, 1 mM THP, and 80 nM ATP in DmB-BSA) and incubated for at least 5 minutes on ice. 2 μL short microtubules are thawed from a frozen aliquot of short microtubules prepared as described in Materials and Methods. MiCA capture bead is prepared by mixing 2 μL short microtubules with 8 μL PEG-amine bead pellet (10 mg/mL) with its buffer removed. After 5 min incubation, the MiCA capture bead is washed 2x with 8 μL BSA-taxol buffer and reconstituted in 2 μL BSA-taxol buffer to give 3 μL final bead volume. Next, 4 μL kinesin-QD is mixed with 3 μL MiCA capture bead and 1 μL AMP-PNP (8 mM), and then incubated for 5 min at room temperature. The mixture is then washed twice with 8 μL BSA-taxol buffer and 8 μL elution buffer (3 mM ATP in BSA-taxol buffer) is added. After 5 min incubation, the eluant is extracted that yields approximately 100 nM kinesin-QD.

For the gliding assay, long fluorescent microtubules are prepared as in Supporting Information section 5, using HyLite 488 as the fluorescent tubulin. Approximately 0.2 nM kinesin-QD before and after MiCA purification is added to biotin-PEG chamber and left to incubate for 5 min. The chamber is then washed with four chamber volume of BSA-taxol buffer, and imaging buffer containing 1 mM ATP, 10x dilution long microtubules, 1 mM

THP, 20 μM paclitaxel, 50 μM biotin, 10 U/mL pyranose oxidase, 4000 U/mL catalase, 2% glucose is added. The chamber is then imaged on TIRF microscope with exposure time of 2 second on two EMCCD camera, one to collect the QD fluorescence, another to collect the microtubule fluorescence. A set of nanohole images on both cameras are also collected for image registration.

For analysis, a transform function is obtained with the nanohole images, as shown in Supporting Figure S7. The QD images are then transformed so that they are registered with the microtubule images. The microtubule image is binarized, thinned to single pixel, then dilated to give it some width. The location of each QD is found using TrackMate in ImageJ. Binary location of the QDs are then overlaid with binary microtubule images, and QD points that overlap with microtubules for at least 8 frames are considered active.

Force-gliding assay

MiCA purification of kinesin-QD, BSA taxol buffer, long fluorescent microtubules, imaging buffer, and image registration are performed the same way as the microtubule gliding assay experiment in Materials and Methods. Kinesin-QD (2 μL, 80 nM) is mixed with Dig-DNA-Biotin (0.25 μL, 80 nM, 1565 base-pair DNA prepared by PCR of pBR322 plasmid with forward primer conjugated to biotin and reverse primer conjugated to dig). Forward primer sequence is /5BiosG/AC AGC ATC GCC AGT CAC TAT G and reverse primer sequence is /5DiGN/GG GAC CAG AGA AAA ATC ACT CAG G. Both are purchased from IDT-DNA using HPLC for purification. There is ~8x less DNA than kinesin-QD to ensure that kinesin-QD has at most 1 DNA attached. After 10 minutes incubation, 0.2 μL biotin (10 mM) is added to the kinesin-QD-DNA mixture.

To prepare flow chamber, 600 nM Streptavidin is added to fill a biotin-PEG chamber (~1.5 μL volume) and incubated for > 5 minutes. The chamber is then washed with 10 μL DmB-BSA, and then 1.5 μL anti-Dig-biotin (10 nM) is added and incubated for >5 minutes. The chamber is then washed with 5 μL DmB-BSA supplemented with 250 μM biotin to saturate the streptavidin surface with biotin. 2 μL kinesin-QD-DNA (adjusted to 0.1 nM DNA concentration) is then added to the chamber and incubated for >5 minutes. The chamber is then washed with 6 μL BSA-Taxol buffer with 250 μM biotin. Imaging buffer containing long fluorescence microtubules, ATP and oxygen scavenging reagents is then added and the chamber is imaged in a TIRF microscope with green laser and 0.2 second exposure time and 1500 frames.

MiCA purification of DDB-QD

3 μL DDB (~20 nM or ~30 ng/μL dynein) is mixed with 3 μL SA-Qd705 (100 nM) and incubated for >3 hours on ice. 2 μL frozen short microtubules are thawed and warmed with hand, and then mixed with 8 μL PEG-amine beads which has its buffer removed after magnetic pull. The mixture is incubated for 5 min at room temperature, then washed 2x with BSA-taxol buffer. On final wash, 7 μL BSA-taxol buffer is added to make 8 μL final solution. This bead solution is then aliquoted into 3 tubes in increasing volume: 0.4 μL, 1.6 μL and 6 μL, which are labeled as 1x, 4x and 15x beads. The buffers of these aliquots are then removed and 1 μL BSA-taxol is added to each. Next, 2 μL DDB-QD is added to each

bead sample, and the mixtures are left to incubate at room temperature for 10 minutes on an end-to-end rotator. The 3 μL supernatant is then removed and labeled ‘Bind’. The pellet is washed twice with 3 μL BSA-taxol, labeled ‘Wash 1’ and ‘Wash 2’. The final pellet is eluted twice with 3 μL elution buffer (1 mM ATP in BSA-taxol) and 5 min incubation. These are ‘Elute 1’ and ‘Elute 2’.

The Bind, Wash 1 and Wash 2 samples are then mixed with 0.25 μL biotin (10 mM) to saturate all streptavidin binding sites on QD, then flowed into microtubule chambers made from PEG-biotin slide layered with streptavidin and long biotin-fluorescent microtubules. DDB-QDs in these samples will bind to microtubules on the chamber. Elute 1 and Elute 2 are diluted twice in imaging buffer, yielding final solution with 0.6 mM ATP, 1 mM THP, 20 μM paclitaxel, 50 μM biotin, 10 U/mL pyranose oxidase, 4000 U/mL catalase, and 2% glucose in DmB-BSA. These final solutions are then flowed into microtubule chamber. All images are recorded on TIRF microscope after ~5 min from infusion into microtubule chamber. Particle counting is done with TrackMate in ImageJ. Signal to noise ratios (SNR) and precision values are obtained by fitting 2d Gaussians to 16 dots from each Bind and Elute 1 movie. This is done using in-house program in Matlab. Each dot consists of 22 to 200 frames that are 0.5s apart in time. The amplitudes and background noises from the Gaussian fits and raw images are used to compute the SNR and precision values.

Supplementary Material

Refer to Web version on PubMed Central for supplementary material.

Acknowledgements

This was supported in part by NIH grant GM108578 and by NSF grant PHY-1430124 to PRS and to NIH grant GM078097 to KMT.

References

(1). Veigel C; Schmidt CF Moving into the Cell: Single-Molecule Studies of Molecular Motors in Complex Environments. Nat. Rev. Mol. Cell Biol 2011, 12 (3), 163–176. [PubMed: 21326200]

(2). Hirokawa N; Takemura R Biochemical and Molecular Characterization of Diseases Linked to Motor Proteins. Trends Biochem. Sci 2003, 28 (10), 558–565. [PubMed: 14559185]

(3). De Vos KJ; Grierson AJ; Ackerley S; Miller CCJ Role of Axonal Transport in Neurodegenerative Diseases. Annu. Rev. Neurosci 2008, 31 (1), 151–173. [PubMed: 18558852]

(4). Stokin GB; Goldstein LSB Linking Molecular Motors to Alzheimer’s Disease. J. Physiol.-Paris 2006, 99 (2), 193–200. [PubMed: 16459060]

(5). Kumar KRS; Kamei T; Fukaminato T; Tamaoki N Complete ON/OFF Photoswitching of the Motility of a Nanobiomolecular Machine. ACS Nano 2014, 8 (5), 4157–4165. [PubMed: 24680285]

(6). Hiratsuka Y; Tada T; Oiwa K; Kanayama T; Uyeda TQP Controlling the Direction of Kinesin-Driven Microtubule Movements along Microlithographic Tracks. Biophys. J 2001, 81 (3), 1555–1561. [PubMed: 11509368]

(7). Heuvel MGL van den; Dekker, C. Motor Proteins at Work for Nanotechnology. Science 2007, 317 (5836), 333–336. [PubMed: 17641191]

(8). Bakewell DJG; Nicolau DV Protein Linear Molecular Motor-Powered Nanodevices. Aust. J. Chem 2007, 60 (5), 314–332.

(9). Agarwal A; Hess H Biomolecular Motors at the Intersection of Nanotechnology and Polymer Science. Prog. Polym. Sci 2010, 35 (1), 252–277.

(10). Aoyama S; Shimoike M; Hiratsuka Y Self-Organized Optical Device Driven by Motor Proteins. Proc. Natl. Acad. Sci 2013, 110 (41), 16408–16413. [PubMed: 24065817]

(11). Fujimoto K; Kitamura M; Yokokawa M; Kanno I; Kotera H; Yokokawa R Colocalization of Quantum Dots by Reactive Molecules Carried by Motor Proteins on Polarized Microtubule Arrays. ACS Nano 2013, 7 (1), 447–455. [PubMed: 23230973]

(12). Finer JT; Simmons RM; Spudich JA Single Myosin Molecule Mechanics: Piconewton Forces and Nanometre Steps. Nature 1994, 368 (6467), 113–119. [PubMed: 8139653]

(13). Yildiz A; Forkey JN; McKinney SA; Ha T; Goldman YE; Selvin PR Myosin V Walks Hand-Over-Hand: Single Fluorophore Imaging with 1.5-Nm Localization. Science 2003, 300 (5628), 2061–2065. [PubMed: 12791999]

(14). Yildiz A; Tomishige M; Vale RD; Selvin PR Kinesin Walks Hand-Over-Hand. Science 2004, 303 (5658), 676–678. [PubMed: 14684828]

(15). Molloy JE; Burns JE; Kendrick-Jones J; Tregear RT; White DCS Movement and Force Produced by a Single Myosin Head. Nature 1995, 378 (6553), 209–212. [PubMed: 7477328]

(16). Svoboda K; Schmidt CF; Schnapp BJ; Block SM Direct Observation of Kinesin Stepping by Optical Trapping Interferometry. Nature 1993, 365 (6448), 721–727. [PubMed: 8413650]

(17). Block SM Kinesin Motor Mechanics: Binding, Stepping, Tracking, Gating, and Limping. Biophys. J 2007, 92 (9), 2986–2995. [PubMed: 17325011]

(18). Gennerich A; Vale RD Walking the Walk: How Kinesin and Dynein Coordinate Their Steps. Curr. Opin. Cell Biol 2009, 21 (1), 59–67. [PubMed: 19179063]

(19). Sellers JR; Veigel C Walking with Myosin V. Curr. Opin. Cell Biol 2006, 18 (1), 68–73. [PubMed: 16378722]

(20). Kural C; Kim H; Syed S; Goshima G; Gelfand VI; Selvin PR Kinesin and Dynein Move a Peroxisome in Vivo: A Tug-of-War or Coordinated Movement? Science 2005, 308 (5727), 1469–1472. [PubMed: 15817813]

(21). Mehta AD; Rock RS; Rief M; Spudich JA; Mooseker MS; Cheney RE Myosin-V Is a Processive Actin-Based Motor. Nature 1999, 400 (6744), 590–593. [PubMed: 10448864]

(22). Altman D; Sweeney HL; Spudich JA The Mechanism of Myosin VI Translocation and Its Load-Induced Anchoring. Cell 2004, 116 (5), 737–749. [PubMed: 15006355]

(23). Gennerich A; Carter AP; Reck-Peterson SL; Vale RD Force-Induced Bidirectional Stepping of Cytoplasmic Dynein. Cell 2007, 131 (5), 952–965. [PubMed: 18045537]

(24). Svoboda K; Block SM Force and Velocity Measured for Single Kinesin Molecules. Cell 1994, 77 (5), 773–784. [PubMed: 8205624]

(25). Veigel C; Wang F; Bartoo ML; Sellers JR; Molloy JE The Gated Gait of the Processive Molecular Motor, Myosin V. Nat. Cell Biol 2002, 4 (1), 59–65. [PubMed: 11740494]

(26). Nelson SR; Ali MY; Warshaw DM Quantum Dot Labeling Strategies to Characterize Single-Molecular Motors In Single Molecule Enzymology; Methods in Molecular Biology; Humana Press, 2011; pp 111–121.

(27). Muthukrishnan G; Hutchins BM; Williams ME; Hancock WO Transport of Semiconductor Nanocrystals by Kinesin Molecular Motors. Small 2006, 2 (5), 626–630. [PubMed: 17193098]

(28). Seitz A; Surrey T Processive Movement of Single Kinesins on Crowded Microtubules Visualized Using Quantum Dots. EMBO J. 2006, 25 (2), 267–277. [PubMed: 16407972]

(29). Schneider R; Korten T; Walter WJ; Diez S Kinesin-1 Motors Can Circumvent Permanent Roadblocks by Side-Shifting to Neighboring Protofilaments. Biophys. J 2015, 108 (9), 2249–2257. [PubMed: 25954882]

(30). Ori-McKenney KM; Xu J; Gross SP; Vallee RB A Cytoplasmic Dynein Tail Mutation Impairs Motor Processivity. Nat. Cell Biol 2010, 12 (12), 1228–1234. [PubMed: 21102439]

(31). Toba S; Watanabe TM; Yamaguchi-Okimoto L; Toyoshima YY; Higuchi H Overlapping Hand-over-Hand Mechanism of Single Molecular Motility of Cytoplasmic Dynein. Proc. Natl. Acad. Sci 2006, 103 (15), 5741–5745. [PubMed: 16585530]

(32). DeWitt MA; Chang AY; Combs PA; Yildiz A Cytoplasmic Dynein Moves Through Uncoordinated Stepping of the AAA+ Ring Domains. Science 2012, 335 (6065), 221–225. [PubMed: 22157083]

(33). Belyy V; Schlager MA; Foster H; Reimer AE; Carter AP; Yildiz A The Mammalian Dynein-Dynactin Complex Is a Strong Opponent to Kinesin in a Tug-of-War Competition. Nat. Cell Biol 2016, 18 (9), 1018–1024. [PubMed: 27454819]

(34). Vale RD; Reese TS; Sheetz MP Identification of a Novel Force-Generating Protein, Kinesin, Involved in Microtubule-Based Motility. Cell 1985, 42 (1), 39–50. [PubMed: 3926325]

(35). Derr ND; Goodman BS; Jungmann R; Leschziner AE; Shih WM; Reck-Peterson SL Tug-of-War in Motor Protein Ensembles Revealed with a Programmable DNA Origami Scaffold. Science 2012, 338 (6107), 662–665. [PubMed: 23065903]

(36). Belyy V; Hendel NL; Chien A; Yildiz A Cytoplasmic Dynein Transports Cargos via Load-Sharing between the Heads. Nat. Commun 2014, 5, 5544. [PubMed: 25424027]

(37). Verbrugge S; Kapitein LC; Peterman EJG Kinesin Moving through the Spotlight: Single-Motor Fluorescence Microscopy with Submillisecond Time Resolution. Biophys. J 2007, 92 (7), 2536–2545. [PubMed: 17237204]

(38). Reck-Peterson SL; Yildiz A; Carter AP; Gennerich A; Zhang N; Vale RD Single-Molecule Analysis of Dynein Processivity and Stepping Behavior. Cell 2006, 126 (2), 335–348. [PubMed: 16873064]

(39). Yildiz A; Tomishige M; Gennerich A; Vale RD Intramolecular Strain Coordinates Kinesin Stepping Behavior along Microtubules. Cell 2008, 134 (6), 1030–1041. [PubMed: 18805095]

(40). Sikora A; Canova FF; Kim K; Nakazawa H; Umetsu M; Kumagai I; Adschiri T; Hwang W; Teizer W Behavior of Kinesin Driven Quantum Dots Trapped in a Microtubule Loop. ACS Nano 2015, 9 (11), 11003–11013. [PubMed: 26426418]

(41). Warshaw DM; Kennedy GG; Work SS; Krementsova EB; Beck S; Trybus KM Differential Labeling of Myosin V Heads with Quantum Dots Allows Direct Visualization of Hand-Over-Hand Processivity. Biophys. J 2005, 88 (5), L30–L32. [PubMed: 15764654]

(42). Berensmeier S Magnetic Particles for the Separation and Purification of Nucleic Acids. Appl. Microbiol. Biotechnol 2006, 73 (3), 495–504. [PubMed: 17063328]

(43). Safarik I; Safarikova M Magnetic Techniques for the Isolation and Purification of Proteins and Peptides. Biomagn. Res. Technol 2004, 2, 7. [PubMed: 15566570]

(44). Fields G Methods for Removing the Fmoc Group In Peptide Synthesis Protocols; Pennington M, Dunn B, Eds.; Methods in Molecular Biology; Humana Press, 1995; pp 17–27.

(45). Grover R; Fischer J; Schwarz FW; Walter WJ; Schwille P; Diez S Transport Efficiency of Membrane-Anchored Kinesin-1 Motors Depends on Motor Density and Diffusivity. Proc. Natl. Acad. Sci 2016, 113 (46), E7185–E7193. [PubMed: 27803325]

(46). McKenney RJ; Huynh W; Tanenbaum ME; Bhabha G; Vale RD Activation of Cytoplasmic Dynein Motility by Dynactin-Cargo Adapter Complexes. Science 2014, 345 (6194), 337–341. [PubMed: 25035494]

(47). Huynh W; Vale RD Disease-Associated Mutations in Human BICD2 Hyperactivate Motility of Dynein–Dynactin. J Cell Biol 2017, 216 (10), 3051–3060. [PubMed: 28883039]

(48). Selvin PR; Lougheed T; Hoffman MT; Park H; Balci H; Blehm BH; Toprak E Fluorescence Imaging with One-Nanometer Accuracy (FIONA). Cold Spring Harb. Protoc 2007, 2007 (10), pdb.top27.

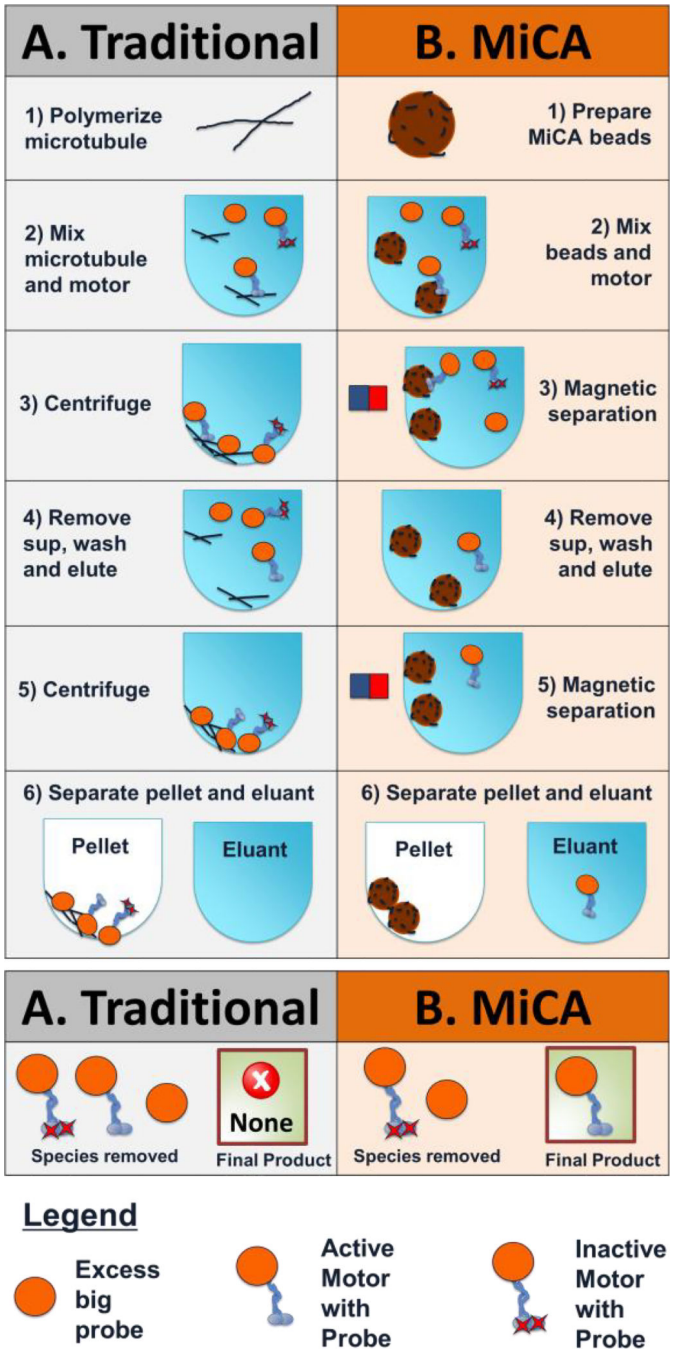

Figure 1:

Comparison between (A) traditional microtubule affinity and (B) MiCA purification for isolation of motors bound to big probe. The magnetic separation (step 3 and 5) for MiCA purification replaces centrifugation used in traditional purification. MiCA purification enables separation of active motors attached to large probes from inactive motors and excess probes, which is not possible with traditional purification.

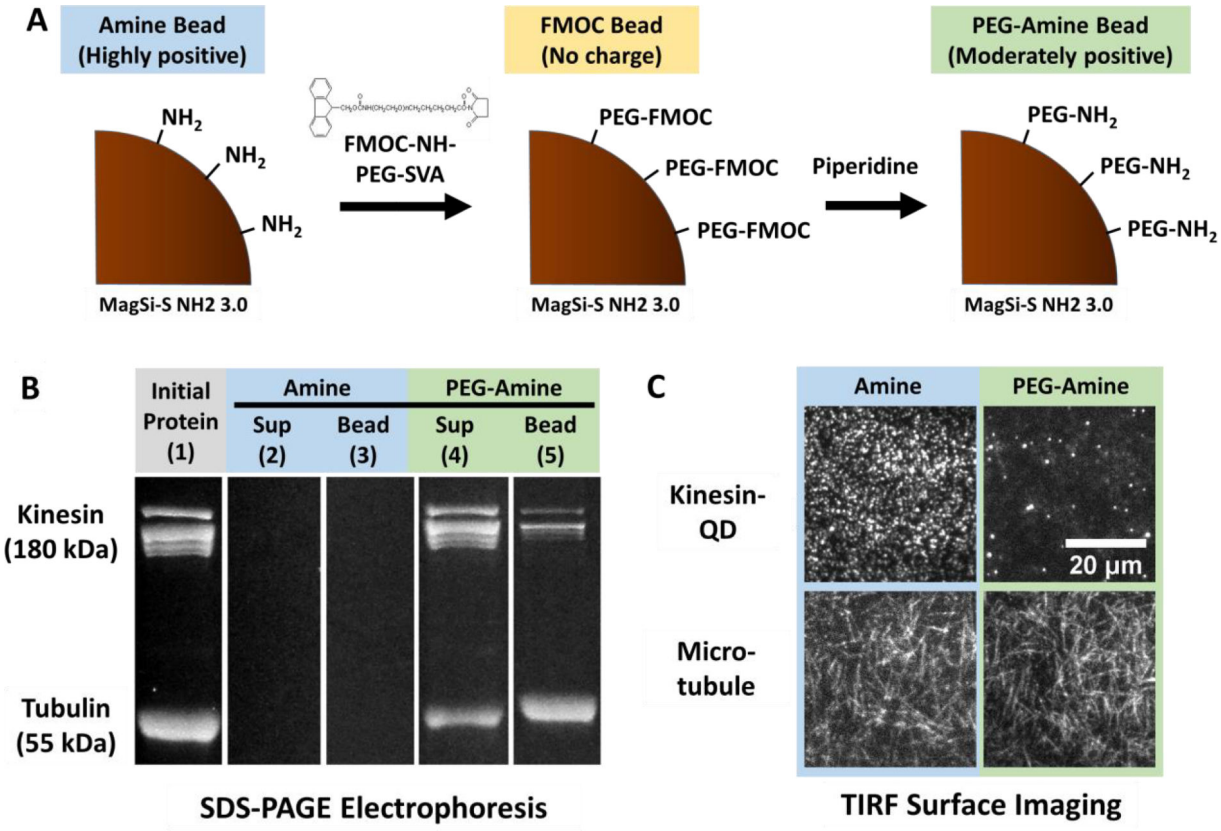

Figure 2:

(A) Synthesis of PEG-amine magnetic bead from commercial amine magnetic bead. For MiCA purification to work, the bead should bind strongly to microtubules, but not to kinesin, a property that PEGylated amine-beads have, but not amine-beads. PEGylation is done by reacting commercial 3.0 μm amine bead (MagSi NH2 3.0 from Amsbio LLC) with FMOC-PEG3400-SVA (Laysan Bio, Inc.) to form PEG-FMOC bead. The FMOC group is then deprotected with piperidine to yield PEG-Amine bead. (B) To show that the PEG-amine beads bind to microtubules but not kinesin, we mix the beads with microtubules or kinesin and monitor their binding to the beads through SDS-PAGE electrophoresis. The gel image shows the initial amount of kinesin and tubulin before mixing with beads (lane 1), the amount left in the supernatant after mixing (lane 2 or 4), and the amount released from the bead after mixing with SDS detergent and incubated at 95°C (lane 3 or 5). Amine-beads bind very strongly to kinesin and microtubules that no protein is left in the supernatant shown on lane 2 and no protein is released from bead shown on lane 3. PEG-amine beads preferentially binds to microtubules but not kinesin, shown in lane 5 where a small fraction of kinesin and a large amount of microtubules bind to the bead, and lane 4 showing that the majority of kinesin and a small fraction of microtubules are left in the supernatant after binding to PEG-amine bead. (C) TIRF surface imaging of kinesin-QD and fluorescent microtubules binding to amine and PEG-amine functionalized on glass coverslip surface. Both surfaces bind to microtubules equally well, but the amine surface binds much more to the kinesin-QD than the PEG-amine surface.

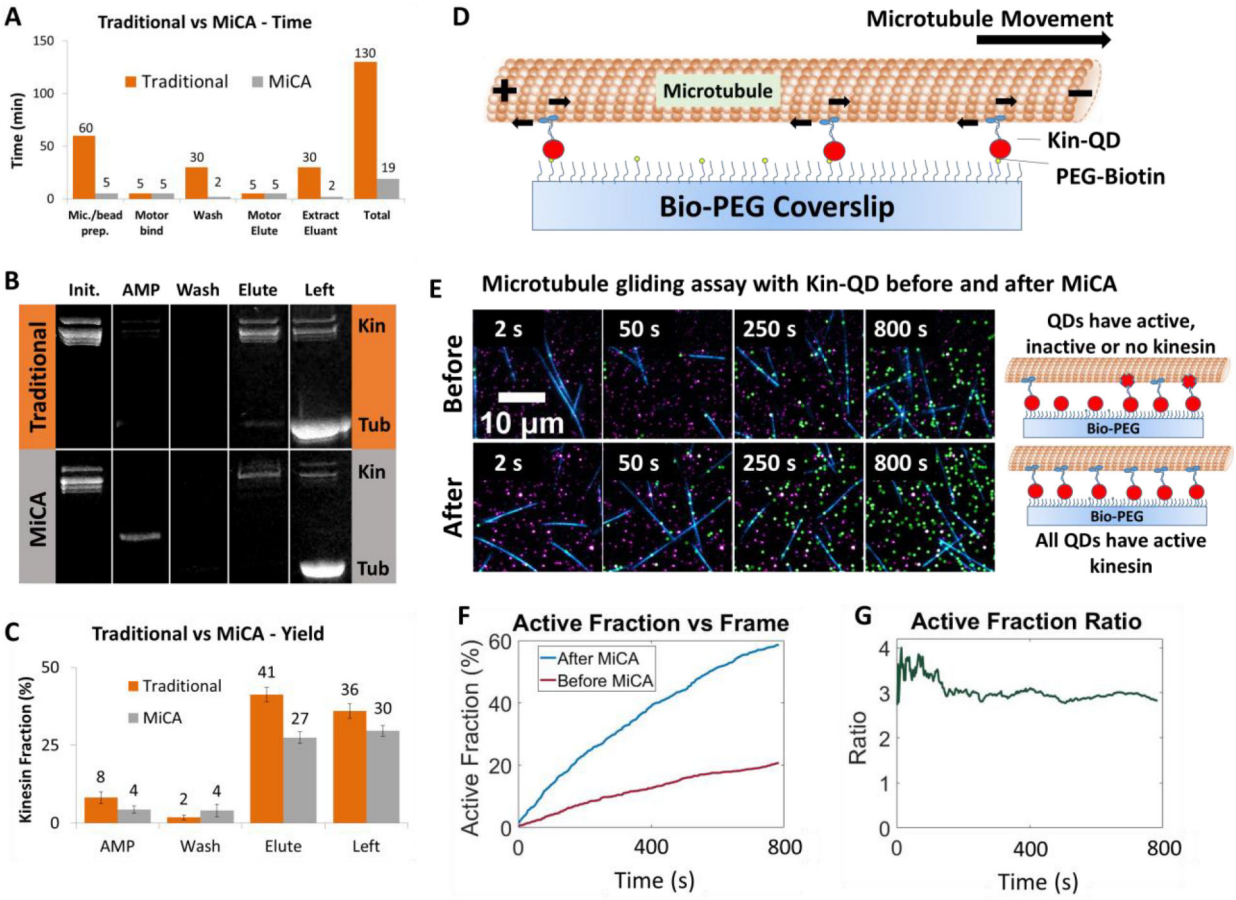

Figure 3:

(A) Purification time comparison between traditional affinity vs MiCA purification. MiCA purification allows seven times reduction in total preparation time, from 130 min to 19 min. (B-C) Yield comparison between traditional affinity and MiCA purification. The quantity of kinesin at each bind (AMP), wash, elute and leftover phases are tracked. Very small amount of kinesin is seen in the bind and wash phase, showing that kinesin is efficiently bound to microtubules/ MiCA capture bead. Kinesin yield with MiCA (27% in elute) is 1.5x less than that for traditional affinity purification (41%). The error bars represent standard error of the mean (standard deviation divided by square-root of sample size) obtained from gel results of 2–5 experiments. (D) Schematic diagram for microtubule gliding assay. Kinesin-streptavidin-QDs purified using MiCA attach to biotin-PEG coverslip. Imaging buffer containing microtubules and ATP are then flowed in, and microtubules will glide on top of and driven by kinesin. Kinesin walk towards plus end of microtubule (left) while microtubule moves in the opposite direction (right) (E) Raw data showing microtubule gliding over kinesin-QD at 2, 50, 250 and 800 seconds before and after MiCA purification, with schematic diagram shown on right. Before MiCA purification, ~40% QDs have no kinesin and some kinesin-QDs are inactive. These QDs will not be able to move microtubule. QD fluorescence is shown in magenta and microtubule in blue. QDs with active kinesin with prior microtubule contact are post-marked with green. Over time, more QDs with active kinesin contacted microtubule and are marked green. (F) Fraction of QDs with

active kinesin before and after MiCA. At the end of experiment, as many as 60% of QDs after MiCA are active, compared to ~20% before MiCA. Across all time period, the fraction of QDs with active kinesin after MiCA is ~3 times higher than before MiCA, as shown in panel (G).

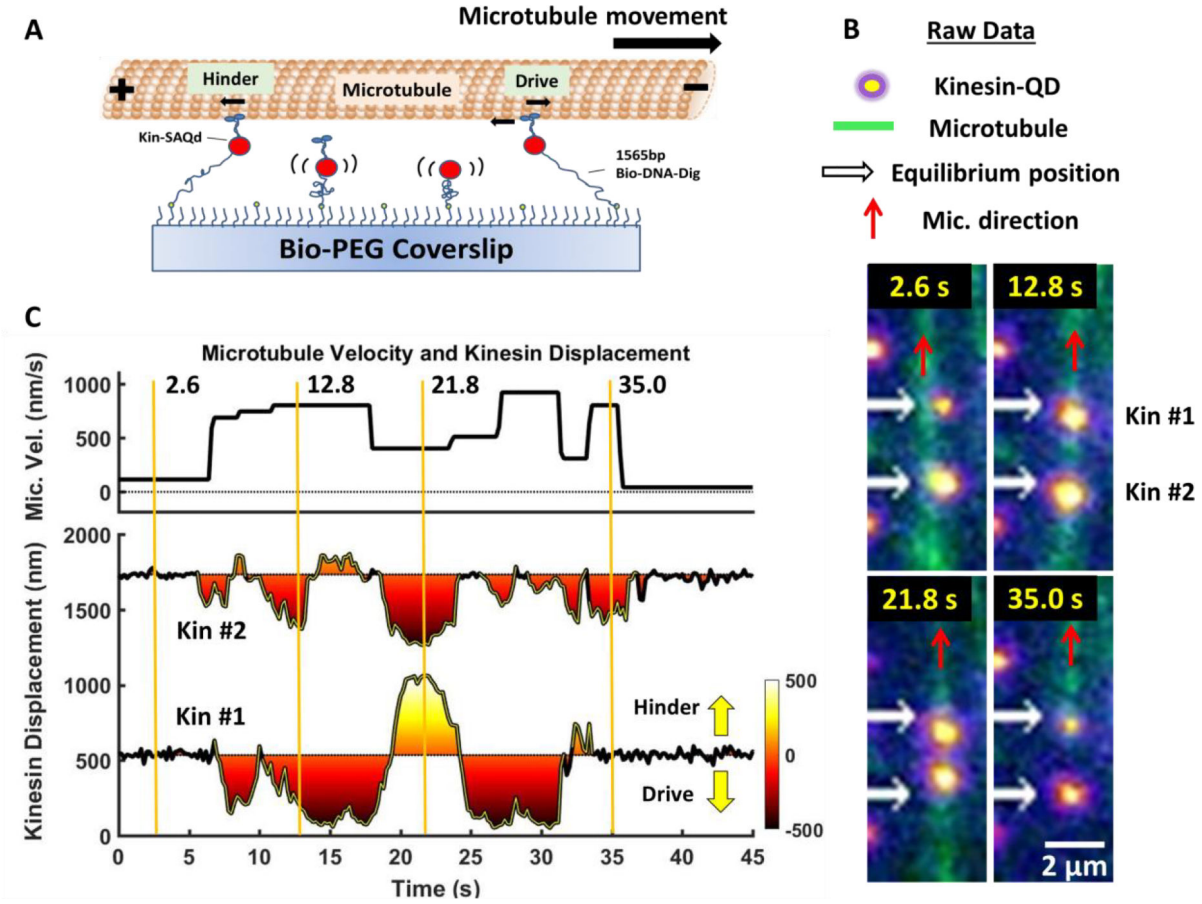

Figure 4:

MiCA purification enables force-gliding assay for parallel detection of forces from multiple kinesin. (A) Schematic diagram of force gliding assay. Kinesin-QD purified with MiCA is attached to biotin-PEG coverslip through 1565 base-pair DNA. DNA acts as a spring that allows force detection of kinesin-QD as it drives or hinders movement of microtubule. Driving kinesin moves in the opposite direction of microtubule, while hindering kinesin moves in the same direction. (B) Snippets of force-gliding assay at 2.6, 12.8, 21.8 and 35.0 s taken from Supplementary Movie S4. Two kinesin move microtubule (green). White arrows show equilibrium kinesin positions. Red arrow shows the direction of microtubule movement. (C) Plots showing microtubule velocity and kinesin positions over time. Time-points at 2.6, 12.8, 21.8 and 35.0 s corresponding to the images in (B) are marked with yellow vertical line. At 2.6 s, microtubule velocity is ~0 nm/s and no kinesin is attached. At 12.8 s, microtubule velocity increases to 800 nm/s when both kinesin are driving (downward displacement from equilibrium). At 21.8 s, top kinesin remains driving, while bottom kinesin hinders microtubule, causing microtubule velocity to fall to 400 nm/s. At 35.0 s, microtubule glides past bottom kinesin, and top kinesin becomes the sole driver, moving microtubule at 800 nm/s.

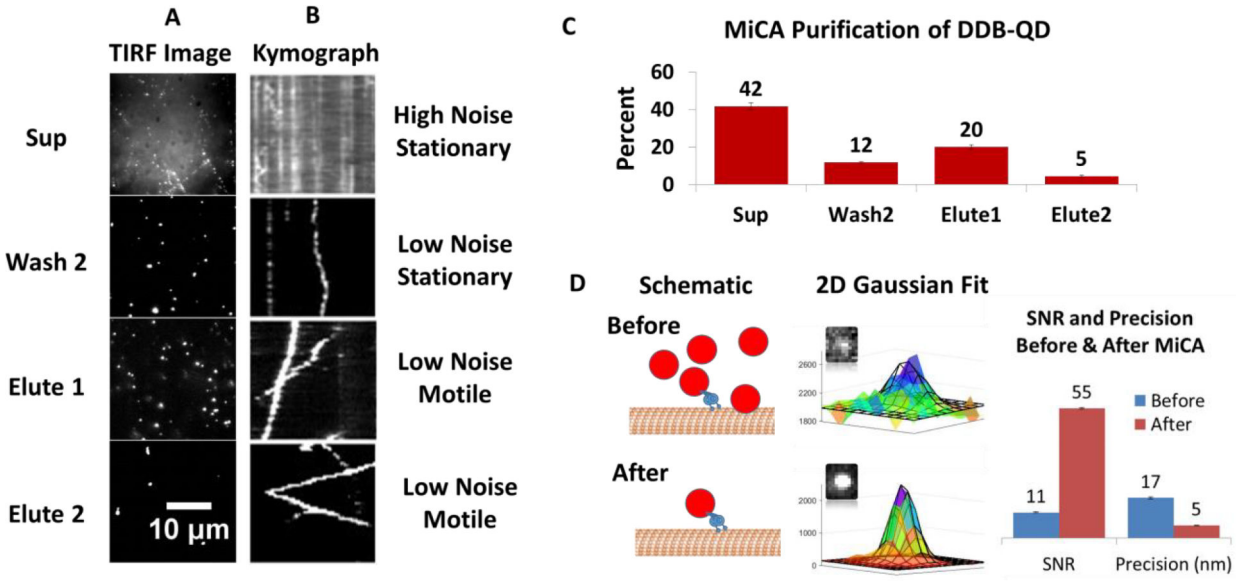

Figure 5:

MiCA purification of DDB-QD. (A-B) TIRF images and kymographs of DDB-QD purification. The amount of DDB-QD left after binding to MiCA capture beads (Sup), left in second wash (Wash 2), and eluting through first and second elution (Elute 1 and 2) are shown in (A) and quantified in (C). Total yield including Elute 1 and 2 is 25%. Free QDs and unbound DDB-QDs contribute to high background noise in Sup. After 2 wash cycles, they are removed, shown by the low background noise in Wash 2, Elute 1 and Elute 2. (B) Kymographs showing DDB-QDs to be stationary or diffusive in Sup and Wash 2, but processive in Elute 1 and 2. This is also shown in Supporting Movie S2. Panel (D) compares the signal to noise (SNR) and precision obtained from QDs before MiCA (Sup) and after MiCA (Elute 1). High background before MiCA causes low SNR (5x less than after MiCA) and poor localization precision (~3x worse than after MiCA). 7–16 frames are collected for yield quantification in panel (C). 1500–1800 QD frames are collected to quantify the SNR and precision in panel (D).